Coordination Polymers

DOI: 10.1002/ange.200704349

Crystal-to-Crystal Transformation between Three Cu^{I} Coordination Polymers and Structural Evidence for Luminescence Thermochromism**

*Tae Ho Kim, Yong Woon Shin, Jong Hwa Jung, Jae Sang Kim, and Jineun Kim**

Recently, there has been considerable interest in the structural and photophysical properties of mono- and polynuclear complexes of transition metals in oxidation states having the d^{10} electronic configuration.[1] Particularly interesting among these are complexes of Cu^{I}, which not only show a great variety of structural forms but are also often brightly luminescent even at room temperature. The luminescence associated with attractive Cu···Cu (cuprophilic) interactions[2] has been of great interest, both from experimental[3] and theoretical[4] perspectives. Such complexes show an unusual wealth of geometries and stoichiometries because of the relatively small energy difference between the various polymorphs, depending on synthetic conditions.[5] In addition, a number of Cu^{I} coordination polymers based on copper(I) iodide and bidentate ligands have been synthesized by self-assembly reactions.[6] The structures of self-assembled coordination polymers depend on a delicate balance between alternative conformations of the organic ligands and on the nature of the metals and anions,[7] as well as the solvent employed.[5c,8] Our interest in Cu^{I} coordination chemistry is mainly focused on thioether ligands.[6] The continuing interest in the S-donor ligands and the scant research on their copper(I) complexes prompted us to investigate the possibility of diverse structures and photophysical properties of copper(I) complexes with a new bis-thioether ligand, namely, 2-(cyclohexylthio)-1-thiomorpholinoethanone (**L**). Although a number of studies on the luminescence thermochromism of cubane-like clusters Cu_4X_4 (X = halogen) have been reported,[1a,3a–d] there was no direct evidence that a change in Cu···Cu distance is responsible for luminescence thermochromism. Herein we report on the synthesis, crystal structures, crystal-to-crystal transformation,[9] and luminescent properties of coordination polymers based on Cu^{I} and **L**.

Ligand **L** was synthesized by the literature method (Scheme S1 in the Supporting Information; crystal data of **L** are listed in Table S1, and an ORTEP view is shown in Figure S1).[6b]

Self-assembly reaction between CuI and **L** under appropriate conditions produced three coordination polymers: yellow nonluminescent **1**, orange luminescent **2**, and green luminescent **3** (Scheme 1). The reaction of CuI and **L** in 1:1 molar ratio at room temperature yielded a product with the formula $[Cu_2I_2\mathbf{L}_2]_n$ (**1**). Crystalline $[Cu_4I_4\mathbf{L}_2]_n$ (**2**) was also

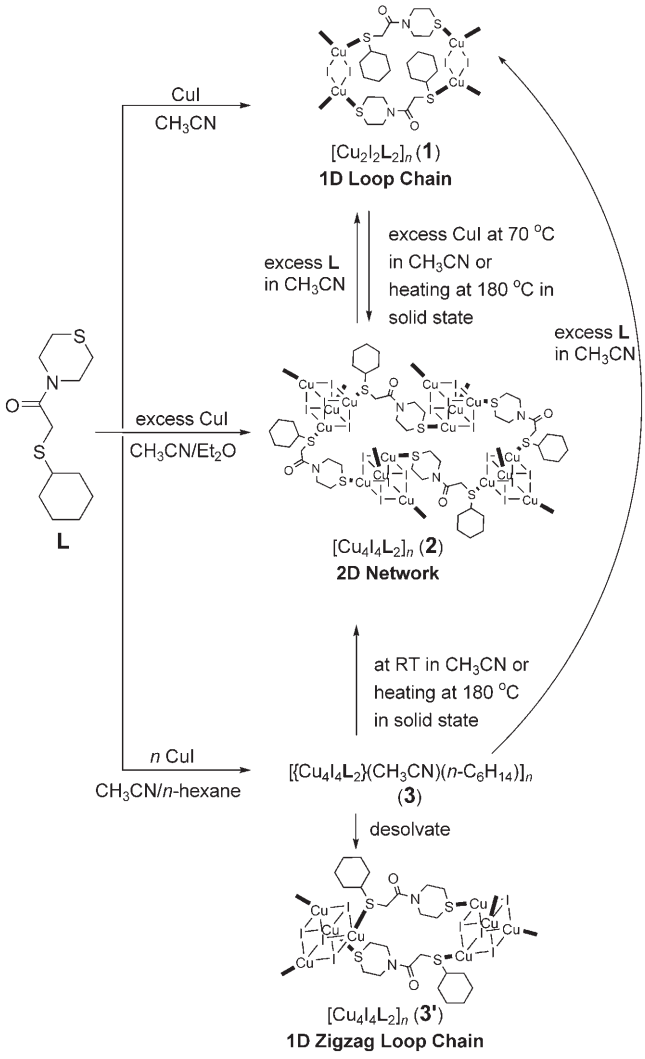

Scheme 1. Syntheses and structural transformations of **1**, **2**, and **3**.

[*] Dr. T. H. Kim, Prof. J. H. Jung, Prof. J. S. Kim, Prof. J. Kim
Department of Chemistry (BK21) and
Research Institute of Natural Science
Gyeongsang National University
900 Gajwa-dong, Jinju 660-701 (South Korea)
Fax: (+82) 55-758-5532
E-mail: jekim@gnu.ac.kr
Dr. Y. W. Shin
Test&Analytical Laboratory
Korea Food&Drug Administration
123-7 Yongdang-dong, Busan 608-829 (South Korea)

[**] T.H.K. was supported by the BK21 program.

Supporting information for this article is available on the WWW under http://www.angewandte.org or from the author.

obtained as a minor product after polymer **1** was crystallized from a solution of CuI and **L** in 2:1 molar ratio. Polymer **2** was also prepared by addition of diethyl ether under conditions of excess CuI. Crystals of $[\{Cu_4I_4\mathbf{L}_2\}\cdot CH_3CN\cdot n\text{-}C_6H_{14}]_n$ (**3**) grew from the boundary between immiscible acetonitrile solution and a layer of *n*-hexane (Figures S2 and S3 in the Supporting Information). In this case, **1** was formed in acetonitrile solution with 1:1 ratio, while **2** was formed in acetonitrile solution with *n*:1 ratio ($n \geq 2$; crystallographic data and perspective views of the structures of **1**–**3** are given in the Supporting Information, Tables S2–S4 and Figures S4–S6, respectively).

In **1**, rhombohedral Cu_2I_2 clusters are linked by the ligands to form a polymeric one-dimensional (1D) loop chain. Structural analysis of **2** revealed 2D undulating polymeric networks with Cu_4I_4 cluster nodes. Although the quality of the single-crystal X-ray data of **3** was lower due to molecules of solvation (acetonitrile and *n*-hexane), the structure of **3** was also determined to be a 1D zigzag loop-chain polymer with Cu_4I_4 cluster nodes. Crystals of **3** lose the solvent at room temperature to yield green luminescent $[Cu_4I_4\mathbf{L}_2]_n$ (**3′**). The 1D loop zigzag polymer **3** transforms into 2D network polymer **2**. Two S donor atoms of **L** in **2** and **3** are on the same side (*syn* conformation) and opposite sides (*anti* conformation) of the amide bond plane, respectively (see Figure S7 in the Supporting Information). It seems that sonication and loss of solvent from **3** led to a change in sulfur conformation from *anti* to *syn*. Thus, S2 (or S4) in **3** can bind to neighboring cubane clusters of other loop chains to form the 2D network structure **2** (Figures S5, S6, and S8 in the Supporting Information). Note that Cu2, Cu4, I2, and I4 positions in **2** are exchanged with respect to those of **3**. As shown in Scheme 1, polymer **1** was transformed into polymer **2** in acetonitrile solution with an excess of CuI at about 70 °C under sonication conditions. On the other hand, polymer **2** was slowly or immediately transformed into polymer **1** in acetonitrile solution with excess **L** under static or sonication conditions, respectively. After **3** sank to the bottom from the boundary surface (Figure S2c in the Supporting Information), **3** transformed into **1** or **2** depending on the solution composition ($n = 1$ and $n \geq 2$, respectively), and the reverse transformation was not possible. Besides the transformation in solvent, crystal-to-crystal transformation without solvent on heating **1**, **2**, or **3** (**3′**) at above 180 °C resulted in polymer **2**. Powder X-ray diffraction (PXRD) patterns for **1**, **2**, and **3** (**3′**) before and after heating are shown in Figure 1 d and e, respectively. After heating, the PXRD patterns of **1** and **3′** are the same as that of **2**, and no change occurred for **2**. In addition, **1**, **2**, and **3′** after heating emitted orange light (Figure 1 c) like **2**. The change in photoluminescence (Figure 1 a–c) agrees with the change in PXRD patterns. After heating, the luminescence spectra from all samples are the same as the spectrum of **2** before heating. Therefore, it is concluded that **2** has the highest thermal stability. (Luminescence spectra before and after heating are shown in Figure S9 in the Supporting Information.)

Copper ions in **1** have distorted tetrahedral environment with two iodido ligands and two sulfur donors in the coordination shell. The Cu···Cu distance (2.98 Å) is longer than the sum of the van der Waals radii (2.80 Å),[10] and thus implies no cuprophilic interaction. The Cu–S (2.278–2.531 Å) and Cu–I bond lengths (2.503–2.972 Å) are within the range of known values.[11]

The single-crystal X-ray data for **2** and **3** were collected at four different temperatures to elucidate the relation between luminescence thermochromism and Cu···Cu distance. Crystalline **3** was unstable at room temperature owing to loss of solvent from the crystals. The Cu···Cu distances of **2** and **3** at different temperature are listed in Table 1. A significant structural feature of **2** is the relatively short Cu···Cu distances, which are shorter than the sum of the van der Waals radii. The Cu···Cu distances decrease with decreasing temperature,

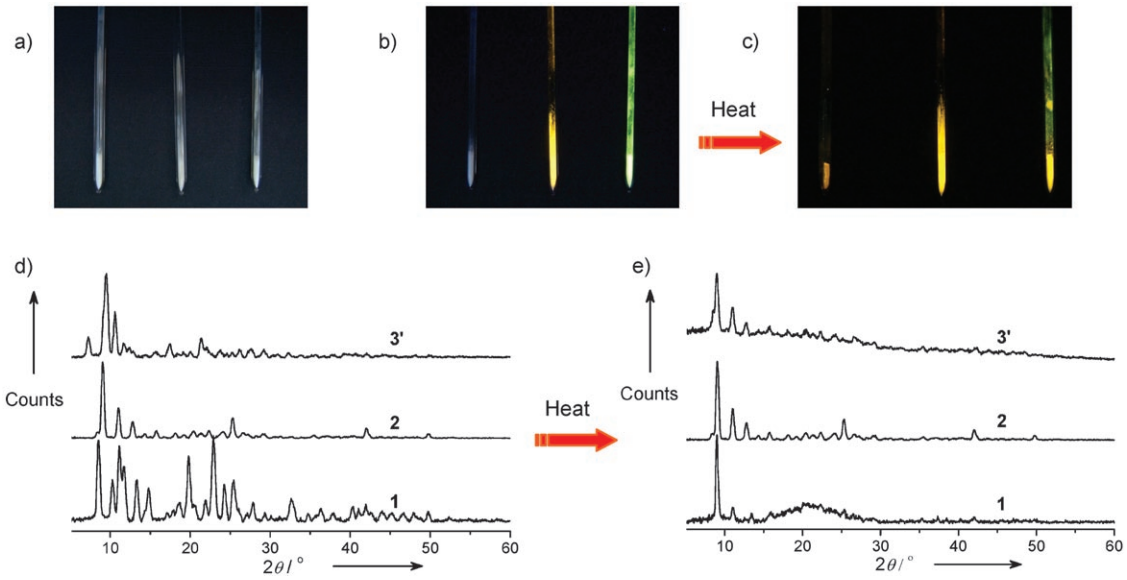

Figure 1. Photographs of **1**, **2**, and **3′** before heating without (a) and with (b) UV irradiation, and after heating with UV irradiation (c). Powder X-ray diffraction patterns of **1**, **2**, and **3′** before (d) and after (e) heating.

Table 1: Cu···Cu distances [Å] in **2** and **3** at four different temperatures.

	298 K[a]	223 K	173 K	123 K
2				
Cu1···Cu3	2.833(2)	2.8052(17)	2.7878(13)	2.7733(10)
Cu1···Cu2	2.789(2)	2.7642(17)	2.7513(13)	2.7403(11)
Cu3···Cu4	2.755(2)	2.7446(17)	2.7400(13)	2.7410(10)
Cu2···Cu3	2.740(2)	2.7267(17)	2.7182(13)	2.7111(11)
Cu1···Cu4	2.625(2)	2.6213(18)	2.6221(14)	2.6292(11)
Cu2···Cu4	2.631(2)	2.6169(17)	2.6107(13)	2.6079(11)
3				
Cu2···Cu4	2.814(3)	2.7930(13)	2.7809(11)	2.7713(10)
Cu1···Cu2	2.815(3)	2.7871(13)	2.7752(11)	2.7652(10)
Cu3···Cu4	2.760(3)	2.7469(13)	2.7344(11)	2.7235(10)
Cu1···Cu4	2.748(3)	2.7321(12)	2.7175(11)	2.7030(10)
Cu2···Cu3	2.736(3)	2.7234(13)	2.7091(11)	2.6981(10)
Cu1···Cu3	2.672(3)	2.6594(12)	2.6501(10)	2.6432(10)

[a] Two runs (600 frames for each run) were collected due to crystal decay.

whereas the Cu–S bond lengths are nearly constant (see Table S5 in the Supporting Information). In addition, some other bond lengths (e.g., C15–C16, C3–C4, C5–C6, C1–C6, C1–C2, S2–C11, and N1–C8) increase, though the lattice constants decrease with decreasing temperature. Surprisingly, longer Cu···Cu distances (Cu1···Cu3, Cu1···Cu2) are substantially contracted, whereas shorter Cu···Cu distances (Cu3···Cu4, Cu1···Cu4) show almost no change. This finding can be explained in terms of fast contraction of the cubane-like Cu_4I_4 cluster and distances such as Cu···Cu, C2–C3, and C14–C15, which causes substantial elongation of other bonds (e.g., C15–C16, C3–C4, C5–C6, C1–C6, C1–C2, S2–C11, and N1–C8) in **2**. This effect may be related to the change in the photoluminescence spectrum of **2**. Similar phenomena were observed for **3**, but the biggest change was observed for Cu–I distances (see Table S6 in the Supporting Information).

Coordination polymer **1** did not emit visible light under UV irradiation. Solid-state emission spectra of powders of **2** and **3′** are shown in Figure 2. The emission bands could be assigned to a combination of ligand-to-metal charge-transfer (LMCT) and d–s transitions due to Cu···Cu interaction within Cu_4I_4 clusters according to previous literature.[4a–e,12] The maxima of the emission bands of **2** were observed at 538 and 599 nm ($\lambda_{ex} = 350$ nm) at room temperature and 77 K, respectively. The band shift of about 60 nm for **2** made detection of the color change by the naked eye possible (Figure 2a, inset). The maxima of the emission bands of **3′** were measured at 526 and 538 nm ($\lambda_{ex} = 286$ nm) in the solid state at room temperature and 77 K, respectively. The shift of the emission peak (10 nm) and the bandwidth of **3′** are smaller than those of **2**, so there was no substantial color change (Figure 2b, inset). The band widths are also related to the spread of Cu···Cu distances (0.208 and 0.143 Å for **2** and **3**, respectively), which vary from 2.625(2) and 2.672(3) Å to 2.833(2) and 2.815(3) Å at 298 K for **2** and **3**, respectively (Table 1). Hence, **2** shows broader spectra than **3′**. With decreasing temperature, the intensity of the short-wavelength part (less than ca. 575 and ca. 525 nm for **2** and **3′**, respectively) of the emission spectrum at 298 K decreases. The peak shifts are related to shortening of the

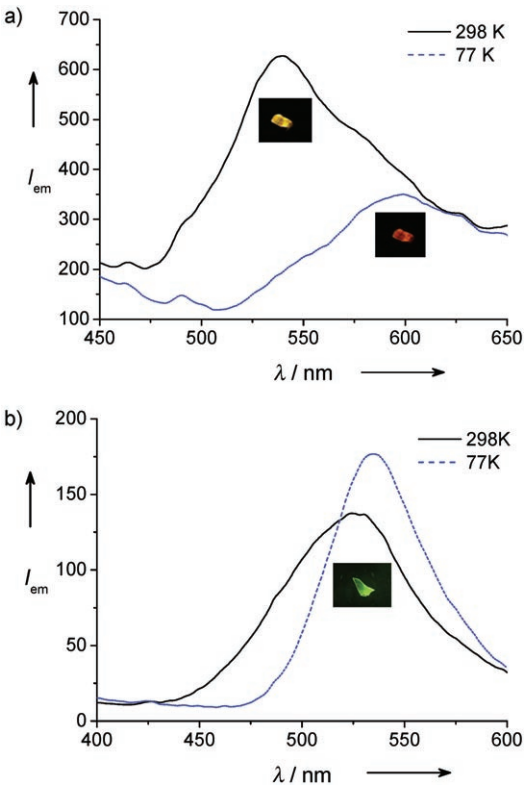

Figure 2. Solid-state luminescence spectra and photographs of **2** (a) and **3′** (b) at 298 (solid line) and 77 K (dashed line).

Cu···Cu distances. According to theoretical works,[4a–e] the Cu–Cu bonds in the excited state (LUMO) are of bonding character. As the temperature decreases, the Cu···Cu distances become shorter, the bonding character increases, and thus the energy levels are lowered. The energy difference between the excited states and the ground state becomes smaller. Thus, shorter-wavelength parts of the emission spectra correspond to transition from excited state of longer Cu···Cu bonds, which disappear with bond shortening. The remaining longer-wavelength parts (600–650 and 525–600 nm regions for **2** and **3′**, respectively) of the emission spectra correspond to transition from excited states of shorter Cu···Cu bonds. Therefore, the wavelength of the emitted light (λ_{max}) increases with decreasing temperature. This is direct evidence that luminescence thermochromism of Cu_4I_4 compounds is caused by temperature-dependent Cu···Cu distances. It seems that no relation exists between Cu–I distances and luminescence thermochromism, since the changes in Cu–I distance in **2** and **3** (from 0.017 and 0.133 Å to −0.005 and −0.102 Å, respectively) are reversed in comparison with the shifts in emission spectra (Tables S5 and S6 in the Supporting Information). However, the Cu–I distances may affect the Cu···Cu distances. The emission intensity at the long-wavelength side does not change for **2**, while it is increased for **3′**. Nonradiative and radiative processes may be involved in **2** and **3′**, respectively. These may be related to population transfer mediated by Cu–I bonds, since the biggest difference between **2** and **3′** is the change in Cu–I distances with temperature (Tables S5 and S6).

In conclusion, we have shown how the solvent and molar ratio of reactants play important roles in the assembly of different coordination polymers from CuI and **L**. Crystal-to-crystal transformations with or without solvent have been discussed. Also, we have demonstrated that temperature-dependent variation of Cu···Cu distance is responsible for the luminescence thermochromism of Cu_4I_4 coordination polymers. Further study of these Cu_4I_4 compounds as well as other CuI coordination polymers is in progress.

Experimental Section

Steady-state luminescence spectra were acquired with a Perkin–Elmer LS 50B spectrophotometer. The excitation and emission spectra were corrected for the wavelength-dependent lamp intensity and detector response, respectively. The pulsed excitation source was generated using the 350-nm line of the xenon lamp for **2** and **3′**. Cooling in temperature-dependent measurements for the solid materials was performed by using a liquid nitrogen tank.

X-ray diffraction experiments were performed in transmission mode on a Bruker GADDS diffractometer equipped with graphite-monochromated $Cu_{K\alpha}$ radiation ($\lambda = 1.54073$ Å). Each diffraction frame was collected at 25° intervals in the 2θ range of 5–60° for 30 s at a detector distance of 15 cm. The two frames were integrated from 5° to 60° and merged.

Single-crystal diffraction data for **L** and **1** at 173 K and for **2** and **3** at four different temperatures (123, 173, 223, and 298 K) were collected on a Bruker SMART CCD diffractometer equipped with graphite-monochromated $Mo_{K\alpha}$ radiation ($\lambda = 0.71073$ Å). The cell parameters for the compounds were obtained from a least-squares refinement of the spot (from 45 collected frames) using the SMART program. The intensity data were processed using the Saint Plus program. All of the calculations for the structure determination were carried out using the SHELXTL package (version 5.1).[13] Absorption corrections were applied by using XPREP and SADABS.[14] In most cases, hydrogen positions were input and refined in a riding manner along with the attached carbon atoms. CCDC 660759–660768 contain the supplementary crystallographic data for this paper. These data can be obtained free of charge from The Cambridge Crystallographic Data Centre via www.ccdc.cam.ac.uk/data_request/cif.

Received: September 20, 2007
Revised: November 9, 2007
Published online: December 13, 2007

Keywords: copper · luminescence · metal–metal interactions · S ligands · thermochromism

[1] a) P. C. Ford, E. Cariati, J. Bourassa, *Chem. Rev.* **1999**, *99*, 3625–3647; b) M. Vitale, P. C. Ford, *Coord. Chem. Rev.* **2001**, *219–221*, 3–16.
[2] a) C.-M. Che, Z. Mao, V. M. Miskowski, M.-C. Tse, C.-K. Chan, K.-K. Cheung, D. L. Phillips, K.-H. Leung, *Angew. Chem.* **2000**, *112*, 4250–4254; *Angew. Chem. Int. Ed.* **2000**, *39*, 4084–4088; b) W.-F. Fu, X. Gan, C.-M. Che, Q.-Y. Cao, Z.-Y. Zhou, N. N.-Y. Zhu, *Chem. Eur. J.* **2004**, *10*, 2228- 2236.
[3] a) H. D. Hardt, *Naturwissenschaften* **1974**, *61*, 107–110; b) H. D. Hardt, A. Pierre, *Inorg. Chim. Acta* **1977**, *25*, L59–L60; c) E. Cariati, X. Bu, P. C. Ford, *Chem. Mater.* **2000**, *12*, 3385–3391; d) S. Hu, M.-L. Tong, *Dalton Trans.* **2005**, 1165–1167; e) H. Araki, K. Tsuge, Y. Sasaki, S. Ishizaka, N. Kitamura, *Inorg. Chem.* **2005**, *44*, 9667–9675.
[4] a) K. R. Kyle, C. K. Ryu, J. A. DiBenedetto, P. C. Ford, *J. Am. Chem. Soc.* **1991**, *113*, 2954–2965; b) M. Vitale, W. E. Palke, P. C. Ford, *J. Phys. Chem.* **1992**, *96*, 8329–8336; c) M. Vitale, C. K. Ryu, W. E. Palke, P. C. Ford, *Inorg. Chem.* **1994**, *33*, 561–566; d) A. Vega, J.-Y. Saillard, *Inorg. Chem.* **2004**, *43*, 4012–4018; e) F. D. Angelis, S. Fantacci, A. Sgamellotti, E. Cariati, R. Ugo, P. C. Ford, *Inorg. Chem.* **2006**, *45*, 10576–10584; f) C. Mealli, S. S. M. C. Godinho, M. J. Calhorda, *Organometallics* **2001**, *20*, 1734–1742.
[5] a) C. Näther, M. Wriedt, I. Jess, *Inorg. Chem.* **2003**, *42*, 2391–2397; b) C. Näther, I. Jess, *Inorg. Chem.* **2003**, *42*, 2968–2976; c) J.-P. Zhang, Y.-Y. Lin, X.-C. Huang, X.-M. Chen, *Dalton Trans.* **2005**, 3681–3685.
[6] a) T. H. Kim, K. Y. Lee, Y. W. Shin, S.-T. Moon, K.-M. Park, J. S. Kim, Y. Kang, S. S. Lee, J. Kim, *Inorg. Chem. Commun.* **2005**, *8*, 27–30; b) T. H. Kim, Y. W. Shin, S. S. Lee, J. Kim, *Inorg. Chem. Commun.* **2007**, *10*, 11–14; c) T. H. Kim, Y. W. Shin, J. S. Kim, S. S. Lee, J. Kim, *Inorg. Chem. Commun.* **2007**, *10*, 717–719.
[7] K.-M. Park, I. Yoon, J. Seo, J.-E. Lee, J. Kim, K. S. Choi, O.-S. Jung, S. S. Lee, *Cryst. Growth Des.* **2005**, *5*, 1707–1709.
[8] T. Wu, D. Li, S. W. Ng, *CrystEngComm* **2005**, *7*, 514–518.
[9] a) X. Xue, X.-S. Wang, R.-G. Xiong, X.-Z. You, B. F. Abrahams, C.-M. Che, H.-X. Ju, *Angew. Chem.* **2002**, *114*, 3068–3070; *Angew. Chem. Int. Ed.* **2002**, *41*, 2944–2946; b) I. Jeß, P. Taborsky, J. Pospíšil, C. Näther, *Dalton Trans.* **2007**, 2263–2270; c) J. J. Vittal, *Coord. Chem. Rev.* **2007**, *251*, 1781–1795.
[10] A. J. Bondi, *Phys. Chem.* **1964**, *68*, 441–451.
[11] The values were retrieved from the 2006 edition of the Cambridge Structural Database (Version 5.28).
[12] C. K. Ryu, M. Vitale, P. C. Ford, *Inorg. Chem.* **1993**, *32*, 869–874.
[13] G. M. Sheldrick, Bruker, SHELXTL-PC, Version 5.10, Bruker-Analytical X-ray Services, Madison, WI, **1998**.
[14] G. M. Sheldrick, SADABS Software for Empirical Absorption Correction, University of Göttingen, Göttingen, Germany, **2000**.

